(Received 10 October 2023, Accepted 20 December 2023, Scheduled 25 December 2023)

Multi-Channel Electromagnetic Filters Based on EIT and Fano Resonances through Parallel Segments and Asymmetric Resonators

Moulay Said Khattab[1,*], Tarik Touiss[1], Ilyass El Kadmiri[1,2], Fatima Zahra Elamri[1], and Driss Bria[1]

[1] *Laboratory of Materials, Waves, Energy and Environment*
Team of Waves, Acoustics, Photonics and Materials, Mohamed I University, Oujda, Morocco
[2] *Laboratory of Computer Science and Interdisciplinary Physics, ENSF*
Sidi Mohamed Ben Abdellah University, Fez, Morocco

ABSTRACT: In this study, we investigate electromagnetically induced transparency (EIT) and Fano resonances, focusing on the propagation of electromagnetic waves in a system of parallel waveguides associated with asymmetric resonators. Our design includes five waveguides and two resonators, generating discrete modes influenced by their respective lengths. The EIT resonance is characterized by a prominent transmission peak flanked by two transmission zeros, while the Fano resonance is characterized by a pronounced transmission peak adjacent to a transmission zero. Using the transfer matrix method (TMM), we calculate transmission and reflection rates. Our results indicate that the EIT resonance appears when the resonator lengths show slight differences, whereas the Fano resonance appears when the resonator lengths are identical. Both resonances are sensitive to resonator lengths and permittivity indices. Consequently, the geometrical parameters of the system must be carefully selected according to the application in question, whether waveguiding or multi-channel electromagnetic filtering.

1. INTRODUCTION

Selective filters are based on the interaction between the incoming electromagnetic wave and the materials of the structure components. Many filters are conceivable such as long-pass, short-pass, interference band-pass filters, and color absorptive filters [1, 2]. In particular, the electromagnetic interference filters are advantageous for their high-quality factor and transmission rate. Moreover, selective electromagnetic filters have now been exploited in other applications as multichannel filters, due to their high capacity to simultaneously transmit multiple frequencies over a single transmission line (channel) at the same time without any manual interference.

Electromagnetically Induced Transparency (EIT) and Fano resonances, extensively researched in systems like photonic waveguides [3], offer potential for innovations like electromagnetic switches [4], and sensors [5]. EIT resonances manifest as prominent transmission peaks flanked by two transmission nulls, while Fano resonances appear adjacent to a transmission null. The genesis of these resonances lies in the interference between incoming electromagnetic waves and the structure's eigenmodes. The scientific community has been fervently exploring the nuances and potential applications of these resonances. Numerous photonic and acoustic multichannel filters, tailored for integrated technology, have been proposed. For instance, Ben-Ali et al. delved into a multichannel Frequency Division Multiplexing (FDM) system based on one-dimensional photonic star waveguides [6]. Mouadili et al. experimentally crafted a photonic device leveraging EIT and Fano resonances [7]. Other notable works include investigations by Islam et al. on double slot waveguides [8], El Kadmiri et al. on multi-channel acoustic filters [9], and Khattab et al. on acoustically induced transparency [10, 11].

The results of our study, although they are based on the TMM method, have significant implications for the field of metasurfaces. The exploitation of electromagnetically induced transparency (EIT) and Fano resonances in metasurfaces opens the way to innovative applications in optics and photonics [12–17]. These phenomena can be used to enhance the control of light at the nanoscale, providing opportunities for the development of advanced optical devices such as ultra-selective filters, highly sensitive light sensors, and improved optical communication systems.

In this study, using the transfer matrix method, we embark a theoretical and numerical exploration of EIT and Fano resonances within one-dimensional parallel segments associated with symmetrical or asymmetrical resonators. Our proposed structure, illustrated in Figure 1, comprises segments of different lengths d_i (i = 1–5), complemented by two resonators of lengths d_6 and d_7. Our main objective is to discern the localization of discrete modes and to verify the potential existence of Fano and EIT resonances in configurations with U-shaped resonators.

Our study sheds light on the phenomenon of electromagnetically induced transparency (EIT) and Fano resonances in our proposed structure. EIT manifests itself in our structure as a result of destructive interference between the resonance modes

* Corresponding author: Moulay Said Khattab (mysaidkhattab@gmail.com).

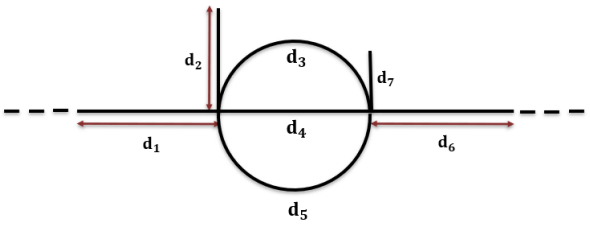

FIGURE 1. Geometric illustration of parallel/serial segments and two grafted resonators located in two different sites.

of the waveguides and resonators. This interference leads to a window of transparency in a specific frequency band, observable when the resonator lengths differ slightly. On the other hand, Fano resonances result from the interaction between a discrete resonance mode created by resonators of identical lengths and a continuous background spectrum offered by the waveguides. This interaction produces a characteristic asymmetrical transmission profile, typical of Fano resonances. These phenomena illustrate the sensitivity of our system to variations in geometrical parameters, underlining the importance of their careful selection for the design of efficient multi-channel electromagnetic filters.

The paper is structured as follows. Section 2 is devoted to a complex analytical calculation of transmission and reflection rates via TMM. Section 3 presents our numerical results and discussions, leading to the conclusion in Section 4.

2. MODEL AND FORMALISM

Our theoretical analysis is based on the formalism of the transfer matrix method, which calculates the transmission rate. The expressions for the electric fields in the segment-resonator are given by:

$$E(x,y)=\begin{cases} E_0(x)=A_0e^{i\alpha_0 x}+B_0e^{-i\alpha_0 x} & \text{for: } x\le 0 \\ E_1(x)=A_1e^{i\alpha_1 x}+B_1e^{-i\alpha_1 x} & \text{for: } 0\le x\le d_1 \\ E_2(y)=C_0e^{i\alpha_2 y}+D_0e^{-i\alpha_2 y} & \text{for: } 0\le y\le d_2 \\ E_s(x)=A_se^{i\alpha_s(x-d_1)} & \text{for: } x\ge d_1 \end{cases} \tag{1}$$

The electric field distribution within each medium is written by the sum of an incident wave and a reflected wave. α_i is the wave number in medium i ($i=0,1,2,s$), and the coefficients A_n and B_n are constants ($n=0,1,s$).

We use the conditions of the passage of electric fields, and we find the transfer matrix of a segment d_1 and a grafted resonator d_2 in the following form:

$$M_1=\begin{pmatrix} C_1-\frac{\alpha_2 S_2}{\alpha_1 C_2}S_1 & -j\frac{S_1}{\alpha_1} \\ -j\alpha_1 S_1-j\frac{\alpha_2 S_2}{C_2}C_1 & C_1 \end{pmatrix} \tag{2}$$

with:

$$C_i = \mathrm{Cos}(\alpha_i d_i),\quad S_i=\mathrm{Sin}(\alpha_i d_i)$$
$$\text{and } \alpha_i = \frac{\omega}{c}\sqrt{\mu_i\varepsilon_i}\,(i=1,2) \tag{3}$$

The transfer matrix of a single segment is:

$$\begin{pmatrix} A_0 \\ B_0 \end{pmatrix} = M_i\begin{pmatrix} A_S \\ B_S \end{pmatrix}=\begin{pmatrix} C_i & -j\frac{S_i}{\alpha_i} \\ -j\alpha_i S_i & C_i \end{pmatrix}\begin{pmatrix} A_S \\ B_S \end{pmatrix}$$
$$=\begin{pmatrix} T_{i,11} & T_{i,12} \\ T_{i,21} & T_{i,22} \end{pmatrix}\begin{pmatrix} A_S \\ B_S \end{pmatrix} \tag{4}$$

We used the admittance matrix to calculate the transfer matrix of the three parallel segments. The segment admittance matrix is:

$$\begin{pmatrix} B_0 \\ B_s \end{pmatrix}=Y_i\begin{pmatrix} A_0 \\ A_S \end{pmatrix}=\begin{pmatrix} y_{i,11} & y_{i,12} \\ y_{i,21} & y_{i,22} \end{pmatrix}\begin{pmatrix} A_0 \\ A_S \end{pmatrix} \tag{5}$$

We use the admittance matrix to calculate the transfer matrix of three parallel segments of lengths d_3, d_4, and d_5:

$$\begin{pmatrix} \mathbf{B}_0 \\ \mathbf{B}_s \end{pmatrix} = \mathbf{Y}_T\begin{pmatrix} \mathbf{A}_0 \\ \mathbf{A}_S \end{pmatrix}=\sum_{i=1}^{3}\mathbf{Y}_i\begin{pmatrix} \mathbf{A}_0 \\ \mathbf{A}_S \end{pmatrix}$$
$$=\begin{pmatrix} \sum_{i=1}^{3}\mathbf{y}_{i,11} & \sum_{i=1}^{3}\mathbf{y}_{i,12} \\ \sum_{i=1}^{3}\mathbf{y}_{i,21} & \sum_{i=1}^{3}\mathbf{y}_{i,22} \end{pmatrix}\begin{pmatrix} \mathbf{A}_0 \\ \mathbf{A}_S \end{pmatrix} \tag{6}$$

The transfer matrix of three parallel segments is given by:

$$\begin{pmatrix} \mathbf{A}_0 \\ \mathbf{B}_0 \end{pmatrix}=\mathbf{M}_2\begin{pmatrix} \mathbf{A}_S \\ \mathbf{B}_S \end{pmatrix}=\frac{-1}{\sum_{i=1}^{3}\mathbf{y}_{i,21}}$$
$$\begin{pmatrix} \sum_{i=1}^{3}\mathbf{y}_{i,22} & \mathbf{-1} \\ \sum_{i=1}^{3}\mathbf{y}_{i,22}\cdot\sum_{i=1}^{3}\mathbf{y}_{i,11} & -\sum_{i=1}^{3}\mathbf{y}_{i,11} \\ -\sum_{i=1}^{3}\mathbf{y}_{i,12}\cdot\sum_{i=1}^{3}\mathbf{y}_{i,21} & \end{pmatrix}\begin{pmatrix} \mathbf{A}_S \\ \mathbf{B}_S \end{pmatrix} \tag{7}$$

The transfer matrix of a segment d_6 and a grafted resonator d_7 is:

$$M_3=\begin{pmatrix} C_6 & -j\frac{S_6}{\alpha_6} \\ -j\alpha_6 S_6-j\frac{\alpha_7 S_7}{C_7}C_6 & C_6-\frac{\alpha_7 S_7}{\alpha_6 C_7}S_6 \end{pmatrix} \tag{8}$$

The global transfer matrix is given by:

$$M_T=M_1\cdot M_2\cdot M_3=\begin{pmatrix} A_T & B_T \\ C_T & D_T \end{pmatrix} \tag{9}$$

The transmission rate is given by:

$$T=\left|\frac{2}{\left[A_T+\alpha_s B_T+\frac{C_T}{\alpha_0}+D_T\left(\frac{\alpha_s}{\alpha_0}\right)\right]}\right|^2 \tag{10}$$

3. RESULTS AND DISCUSSIONS

In this section, we numerically illustrate the propagation of electromagnetic waves through a system containing parallel segments and symmetric/asymmetric resonators (Figure 1). We take the dielectric permittivity of the segments and resonators respectively as $\varepsilon_1 = \varepsilon_2 = 2.3$ (polyethylene) (the materials involved in the structure are identical), and the magnetic permeability of the materials is $\mu_1 = \mu_2 = 1$ (non-magnetic medium). We study the effect of the presence of two resonators in order to obtain two types of resonances (AIT and Fano). The reduced frequency is given by $\Omega = \frac{\omega D}{c}$, which is a dimensionless quantity; D is a unit length; c is the velocity of electromagnetic waves in vacuum; and ω is the pulsation. We find that the real frequency domain depends strongly on the size of the lengths.

3.1. Discrete Modes of a Single Cellule

In this section, our focus is directed towards the eigenmodes of a photonic waveguide system. This system, as depicted in Figure 1, comprises three parallel/serial segments, complemented by two resonators strategically positioned at distinct sites. These components are encapsulated between two semi-infinite segments of identical nature.

In Figure 2, we study the relation between the reduced frequency and the lengths of the parallel segments. For this analysis, we take parameters $d_1 = 1D$, $d_2 = d_7 = 0.46D$, and $d_6 = 1.5D$. The black branches, representing the discrete modes, signify the transmission peaks of our proposed system. It is evident that for each segment length, one or multiple discrete modes emerge, each corresponding to a specific frequency. Intriguingly, as the lengths of the parallel segments are augmented, there is a discernible shift of the discrete modes towards lower frequencies. Concurrently, the quantity of discrete modes also witnesses an upsurge. This observed trend aligns with findings from previous studies on acoustic star waveguide structures, as cited in [10, 11].

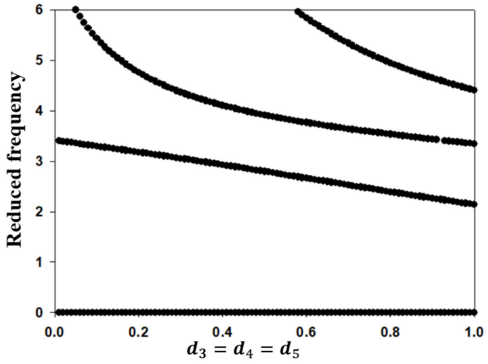

FIGURE 2. Variation of the reduced frequency as a function of the segments lengths $d_3 = d_4 = d_5$.

3.2. Effect of the Identical Resonator

In observation of Figure 3(a), we identify a resonance mode close to a single transmission zero on the right side, a signal characteristic of a Fano resonance. When we increase the lengths of the identical resonators, as seen in cases (b) and (c), the Fano resonance (represented by the maximum transmission peak near a single transmission zero on the right) shifts to lower frequencies. Interestingly, in case (d), the maximum transmission peak is observed near a single transmission zero, but this time on the left-hand side.

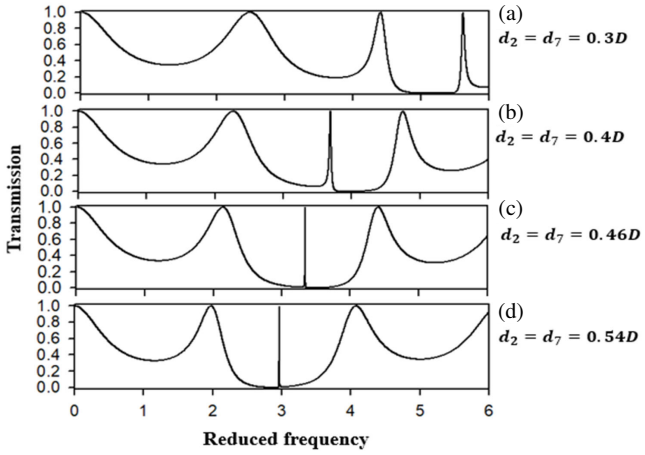

FIGURE 3. Transmission rate as a function of the reduced frequency for identical values of resonators lengths d_2 and d_7.

From these observations, we deduce that the Fano resonance phenomenon occurs when the resonators have equivalent lengths. Moreover, this mode gravitates towards lower frequencies as resonator lengths are varied, notably d_2 and d_7.

3.3. Transmission Spectrum: Effect of EIT Resonance

In the following discussion, we examine Figure 4, which illustrates the variation in transmission rate as a function of reduced frequency. To do this, we have chosen different lengths for the d_7 resonator, while keeping the d_2 resonator length fixed at $0.46D$. In all the cases shown in Figure 4, we observe a transmission peak located between two transmission zeros. This specific resonance feature is recognized as an EIT resonance. Our analysis shows that as the length of the d_7 increases, the EIT resonance shifts to lower frequencies, accompanied by a decreasing quality factor.

3.4. Color Map: Effect of Resonators Lengths d_2 and d_7

To obtain an EIT resonance, it is necessary to choose two resonators of different lengths. For our study, we set $d_1 = 0.5D$, $d_6 = 1.5D$, and $d_3 = d_4 = d_5 = 1D$. In Figure 5(a), with $d_2 = 0.46D$ and $d_7 = 0.54D$, a discernible maximum transmission peak is observed, located between two transmission zeros in the frequency range $\Omega = [3–3.25]$.

To determine the optimal geometrical parameters that produce the highest transmission rate for the EIT resonance, we illustrate, in Figure 5(b), a color map. This map plots the transmission rate in the reduced frequency range of $\Omega = [3–3.25]$ as a function of resonator lengths d_2 and d_7. Each coordinate (d_2, d_7) on this map corresponds to a specific transmission rate. Green corresponds to medium transmission, while dark blue represents minimum transmission. The red regions,

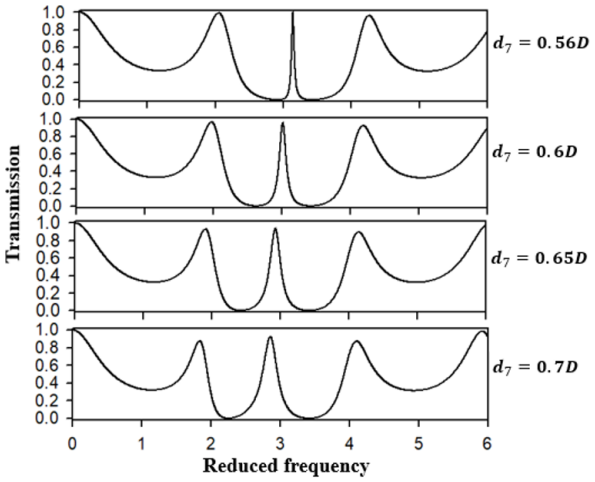

FIGURE 4. Transmission rate as a function of the reduced frequency for different resonators lengths d_7 with $d_2 = 0.46D$.

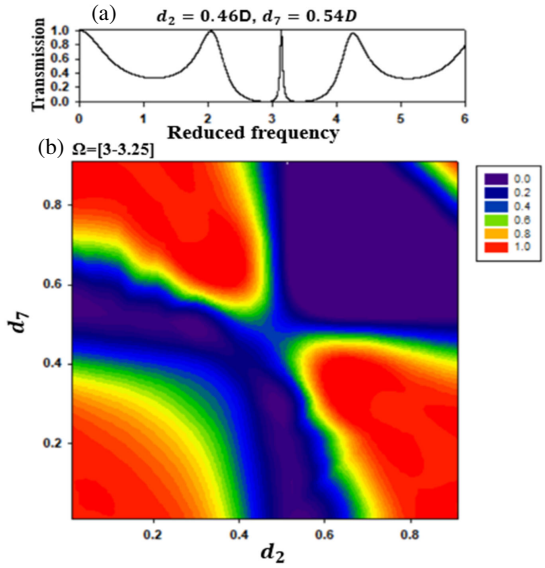

FIGURE 5. (a) Transmission rate as a function of the reduced frequency for $d_2 = 0.46D$ and $d_7 = 0.54D$. (b) Color map of transmission maximum versus the resonators of lengths d_2 and d_7 for $\Omega = [3–3.25]$.

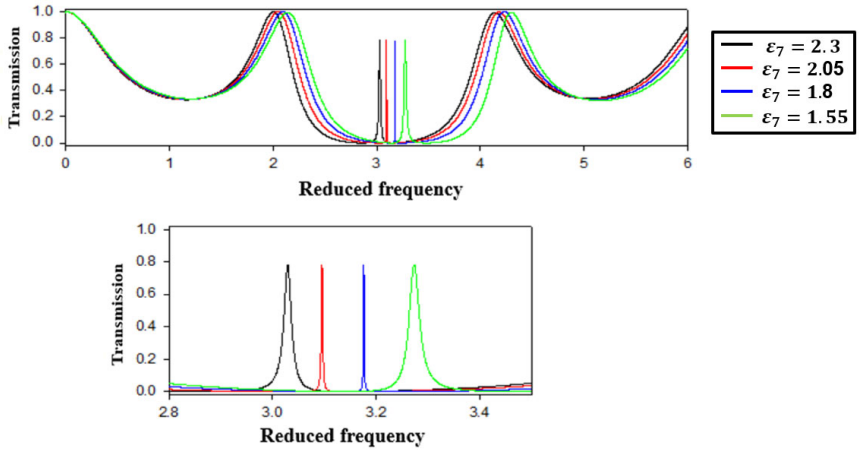

FIGURE 6. Transmission rate as a function of the reduced frequency for different values of ε_7.

on the other hand, indicate high transmission rates for different resonator lengths. In particular, transmission maxima show symmetry around the central axis of resonator lengths.

3.5. Effect of the EIT Resonant with the Resonator Permittivity

The variation permittivity of the resonator has an important effect on the propagation of electromagnetic waves in our proposed system and can be used to improve the performance of the structure. We take $d_1 = d_2 = d_6 = 0.5D$, $d_3 = d_4 = d_5 = 1D$, and $d_7 = 0.55D$, and we vary the permittivity of the resonators ε_7 in order to study the behavior of the EIT resonance. Figure 6 represents the transmission rate as a function of the reduced frequency for different values of ε_7. We notice that the EIT resonance moves to low frequencies when increasing the permittivity ε_7 of the resonator of length d_7 with a step of 0.25.

4. SUMMARY

In this study, using the transfer matrix method, we explored the potential for creating multi-channel electromagnetic filters by taking advantage of Fano and EIT (electromagnetically induced transparency) resonances. We focused on a simple structure comprising five waveguides associated with two asymmetrical resonators. A Fano resonance is characterized by full transmission near zero transmission. Conversely, an EIT resonance is characterized by a peak transmission located between two transmission zeros. The positioning and half-value width of the EIT resonance are highly sensitive to changes in segment and resonator length. Consequently, these parameters must be carefully selected to suit the specific application in question.

REFERENCES

[1] Djavid, M. and M. S. Abrishamian, "Multi-channel drop filters using photonic crystal ring resonators," *Optik*, Vol. 123, No. 2,

167–170, 2012.

[2] Hu, S., L. Li, X. Yi, and C. Yu, "Ultraflat widely tuned single bandpass filter based on stimulated Brillouin scattering," *IEEE Photonics Technology Letters*, Vol. 26, No. 14, 1466–1469, Jul. 2014.

[3] Caselli, N., F. Intonti, F. L. China, F. Biccari, F. Riboli, A. Gerardino, L. Li, E. H. Linfield, F. Pagliano, A. Fiore, and M. Gurioli, "Generalized Fano lineshapes reveal exceptional points in photonic molecules," *Nature Communications*, Vol. 9, No. 1, 396, Jan. 2018.

[4] Limonov, M. F., M. V. Rybin, A. N. Poddubny, and Y. S. Kivshar, "Fano resonances in photonics," *Nature Photonics*, Vol. 11, No. 9, 543–554, 2017.

[5] Limonov, M. F., "Fano resonance for applications," *Advances in Optics and Photonics*, Vol. 13, No. 3, 703–771, Sep. 2021.

[6] Ben-Ali, Y., A. Ghadban, I. E. Kadmiri, Y. Bouchafra, and D. Bria, "Microwave multichannel frequency division multiplexing by defectives star waveguides," *Optical Memory and Neural Networks*, Vol. 31, No. 1, 76–96, 2022.

[7] Mouadili, A., E. H. E. Boudouti, A. Soltani, A. Talbi, A. Akjouj, and B. Djafari-Rouhani, "Theoretical and experimental evidence of Fano-like resonances in simple monomode photonic circuits," *Journal of Applied Physics*, Vol. 113, No. 16, Apr. 2013.

[8] Islam, M., K. M. Dhriti, R. Sarkar, and G. Kumar, "Tunable control of electromagnetically induced transparency effect in a double slot terahertz waveguide," *Optics Communications*, Vol. 483, 126632, Mar. 2021.

[9] El Kadmiri, I., Y. Ben-Ali, Y. Errouas, A. Khaled, and D. Bria, "Multi-channel filters with high performance based on the creation of a geometrical defect in 1D phononic star waveguides structure," *Materials Today: Proceedings*, Vol. 45, No. 8, 7576–7583, 2021.

[10] Khattab, M. S., I. E. Kadmiri, Y. Ben-Ali, A. Khaled, F. Jeffali, and D. Bria, "Propagation of the acoustic waves in a one-dimensional parallel guides and symmetric/asymmetric resonators," *Materials Today: Proceedings*, Vol. 72, 3319–3325, 2023.

[11] Khattab, M. S., Y. Ben-Ali, J. Barkani, J. Yousfi, and D. Bria, "Induced guided acoustic waves in waveguides and resonators," *Materials Today: Proceedings*, Vol. 72, 3398–3403, 2023.

[12] Limonov, M. F., M. V. Rybin, A. N. Poddubny, and Y. S. Kivshar, "Fano resonances in photonics," *Nature Photonics*, Vol. 11, No. 9, 543–554, Sep. 2017.

[13] Wang, D.-C., R. Tang, Z. Feng, S. Sun, S. Xiao, and W. Tan, "Symmetry-assisted spectral line shapes manipulation in dielectric double-Fano metasurfaces," *Advanced Optical Materials*, Vol. 9, No. 4, 2001874, Feb. 2021.

[14] Romain, X., R. Degl'Innocenti, F. I. Baida, and P. Boyer, "Polarization-induced Fano resonances using wire-grid metasurfaces for the THz region," in *Metamaterials, Metadevices, and Metasystems 2020*, Vol. 11460, 30–35, 2020.

[15] Zhao, Z., Z. Gu, R. T. Ako, H. Zhao, and S. Sriram, "Coherently controllable terahertz plasmon-induced transparency using a coupled Fano-Lorentzian metasurface," *Optics Express*, Vol. 28, No. 10, 15 573–15 586, May 2020.

[16] Badri, S. H., H. Soofi, and S. S. Nahaei, "Thermally reconfigurable extraordinary terahertz transmission using vanadium dioxide," *Journal of the Optical Society of America B-Optical Physics*, Vol. 39, No. 6, 1614–1621, Jun. 2022.

[17] Badri, S. H., M. M. Gilarlue, S. S. Nahaei, and J. S. Kim, "High-Q Fano resonance in all-dielectric metasurfaces for molecular fingerprint detection," *Journal of the Optical Society of America B-Optical Physics*, Vol. 39, No. 2, 563–569, Feb. 2022.